



## Study on the adsorption of Ciprofloxacin antibiotic in water using biochar synthesized from pine bark via microwave pyrolysis

Huynh Phuong Thao<sup>1\*</sup>, Nguyen Hai Ha<sup>1</sup>, Tran Thi Hoai Linh<sup>1</sup>, Le Vu Tram Anh<sup>1</sup>,  
 Nguyen Thi To Uyen<sup>1</sup>, Vu Thi Bao Ngoc<sup>1</sup>, Nguyen Phi Ho<sup>2</sup>

<sup>1</sup> Faculty of Chemistry and Environment, Da Lat University, 01 Phu Dong Thien Vuong, Ward 8, Da Lat City, Lam Dong Province

<sup>2</sup> Post-graduate student, Da Lat University, 01 Phu Dong Thien Vuong, Ward 8, Da Lat City, Lam Dong Province

\* Email: [thaohp@dlu.edu.vn](mailto:thaohp@dlu.edu.vn)

### ARTICLE INFO

Received: 22/07/2025

Accepted: 20/09/2025

Published: 30/09/2025

#### Keywords:

Antibiotic removal;  
 Ciprofloxacin;  
 Biochar; pine bark;  
 microwave pyrolysis.

### ABSTRACT

The presence of antibiotic residues in aquatic environments—particularly ciprofloxacin—poses serious risks to ecosystems and public health due to their persistence and ability to promote antimicrobial resistance. This study aimed to synthesize biochar from *Pinus kesiya* bark using microwave-assisted pyrolysis and to evaluate its effectiveness in removing ciprofloxacin from aqueous solutions. The physicochemical characteristics of the biochar were investigated using FT-IR, SEM, EDX, and BET analyses. The optimal pyrolysis condition was determined to be 800 W for 10 minutes, producing a material with a high specific surface area (592.32 m<sup>2</sup>/g) and pore volume (0.197 cm<sup>3</sup>/g), indicating a well-developed porous structure—favorable for adsorption. Adsorption experiments revealed that the maximum ciprofloxacin removal efficiency (90.97%) was achieved at pH 6, with an initial concentration of 20 mg·L<sup>-1</sup> and an equilibrium time of 180 minutes. Kinetic data were well-fitted to the pseudo-second-order model ( $R^2 = 0.9945$ ), suggesting the possibility of chemical interactions between the biochar surface and ciprofloxacin molecules. Additionally, the adsorption process was best described by the Langmuir isotherm model, with a maximum monolayer adsorption capacity ( $q_{max}$ ) of 26.51 mg/g. These findings demonstrate that biochar derived from pine bark is a promising, sustainable, and low-cost adsorbent for the treatment of antibiotic-contaminated water. The biochar synthesized via microwave pyrolysis not only exhibits high efficiency in ciprofloxacin removal but is also environmentally friendly, making it a viable material for wastewater treatment systems, especially those dealing with antibiotic residues from medical and agricultural sources.

### Introduction

Vietnam is among the countries with the highest rates of antibiotic consumption and antimicrobial resistance globally [1]. This alarming situation undermines the effectiveness of treatment regimens and adversely

affects the economy, aquatic ecosystems, and human health. Among various antibiotics, ciprofloxacin—a member of the fluoroquinolone group—is widely used in both human and veterinary medicine due to its broad-spectrum antibacterial activity, high bioavailability, cost-effectiveness, and strong clinical

efficacy [2]. While ciprofloxacin is not effective against viruses and not officially recommended for the treatment of COVID-19, it has been employed in some cases to manage secondary bacterial infections in hospitalized COVID-19 patients [3]. However, a significant portion of ciprofloxacin is excreted unmetabolized from the human body and subsequently enters wastewater systems. Owing to its poor biodegradability and the low removal efficiency of conventional wastewater treatment plants (WWTPs), ciprofloxacin persists in the aquatic environment. Even at low concentrations, it can exert toxic effects on aquatic organisms and more critically, promote the development and spread of antimicrobial resistance (AMR). Given the potential ecological and public health risks, there is an urgent need to develop and implement advanced and efficient technologies for the removal of ciprofloxacin from wastewater and environmental waters [4].

Among various wastewater treatment technologies, adsorption stands out as one of the most promising methods due to its low operational cost, technical simplicity, and high removal efficiency for a wide range of pollutants. In particular, naturally derived adsorbents, especially those obtained from agricultural and forestry by-products, are gaining increasing attention for sustainable water pollution control, owing to their abundance, renewability, biodegradability, and potential for surface modification to enhance performance [5].

In Da Lat, a large portion of pine bark waste remains underutilized—mostly discarded or used as fuel—leading to resource wastage and environmental pollution. Pine bark accounts for approximately 10–15% of a tree's weight and possesses a porous structure rich in complex polymers such as cellulose, hemicellulose, and lignin, with a relatively large surface area. Valorizing this abundant, eco-friendly biomass by converting it into biochar for use as an adsorbent enhances the material's value and contributes to environmental remediation. Compared to conventional pyrolysis, microwave-assisted pyrolysis (MAP) offers several advantages in biochar production, including lower greenhouse gas emissions, higher specific surface area of the resulting biochar, shorter reaction times, and greater energy efficiency. These benefits make MAP an increasingly attractive approach for the sustainable conversion of biomass into high-performance adsorbent materials [6]. Based on this theoretical and practical background, this study titled "Study on the adsorption of ciprofloxacin antibiotic in water using biochar synthesized from pine bark via microwave pyrolysis" was conducted with the

following objectives: (1) to synthesize biochar from *Pinus kesiya* bark using microwave-assisted pyrolysis; (2) to evaluate the ciprofloxacin adsorption capacity of the biochar under various conditions, including pH, initial antibiotic concentration, and contact time; and (3) to investigate the adsorption kinetics and isotherms of the process.

## Experimental and research methods

### *Instruments and equipment:*

UV-Vis spectrophotometer (Jenway, UK); analytical balance with sensitivity of  $10^{-4}$  g (Satorius, Germany); oven (Shellab, UK); magnetic stirrer with heating function (IKA, Germany); pH meter (Inolab 730, Germany); Whatman filter paper with pore size 20–25  $\mu\text{m}$ ; sieves of 125 and 212  $\mu\text{m}$  mesh size; 10 mL polyethylene sample vials; and other standard laboratory glassware.

### *Chemicals:*

Ciprofloxacin 500 mg (Ciprofloxacin (CFC), molecular formula:  $\text{C}_{17}\text{H}_{18}\text{FN}_3\text{O}_3$ ) produced by STADA, Vietnam; HCl, NaOH, and KCl.

### *Synthesis of Biochar from Pine Bark*

Pine bark collected in Da Lat City was pretreated by washing thoroughly and soaking in water for 24 hours to remove adhered impurities. It was then rinsed with distilled water, cut into small pieces of approximately  $2 \times 2$  cm, and dried to constant weight at  $80^\circ\text{C}$  for 24 hours. The pine bark was ground and sieved to obtain a particle size range of 125–212  $\mu\text{m}$ . The material was pyrolyzed under anaerobic conditions in a Nabertherm furnace (Germany) at  $600^\circ\text{C}$ , with a heating rate of  $10^\circ\text{C}/\text{min}$ , and maintained at this temperature for 2 hours. The resulting biochar was stored in a plastic container with a tightly sealed lid and kept in a desiccator at room temperature. The material was dried at  $80^\circ\text{C}$  for 24 hours prior to undergoing microwave-assisted pyrolysis. The pyrolysis process was carried out in a microwave oven at a power of 800 W for 10 minutes. The resulting material was rinsed with distilled water and then dried at  $100^\circ\text{C}$  for 24 hours to obtain the final biochar material, which was designated as BCMAP.

After synthesis, the material was characterized to determine its structural properties. The main functional groups present in the biochar were identified using Fourier-transform infrared spectroscopy (FT-IR), with measurements conducted on a Thermo Nicolet 6700 instrument (USA). The elemental composition (EDX) and surface morphology (SEM) of the biochar were

examined using a Hitachi S-4800 field emission scanning electron microscope (FE-SEM, Japan). The specific surface area (BET) of the biochar was measured using a Nova 4000e instrument (USA).

### Batch Adsorption Experiments

The adsorption capacity of ciprofloxacin onto the synthesized biochar was investigated through batch adsorption experiments. A known mass of biochar ( $0.1000 \pm 0.0001$  g) was added to a 100 mL Erlenmeyer flask containing 50 mL of ciprofloxacin solution with a known concentration. The mixture was stirred at 150 rpm, and after adsorption, the solution was filtered. The remaining ciprofloxacin concentration was determined by UV-Vis spectroscopy.

The following parameters were varied:

Effect of pH: Solution pH was adjusted between 2 and 10 using 0.1 N NaOH or HCl.

Effect of contact time: Stirring times ranged from 10 to 240 minutes.

Effect of initial concentration: Ciprofloxacin concentrations ranged from 20 to 100 mg/L.

The residual concentration ( $C_e$ ) was measured at  $\lambda = 285$  nm. Adsorption capacity  $q_e$  (mg/g) and the adsorption efficiency (H) was calculated using Equation:

$$q_e = \frac{(C_0 - C_e) \times V}{m}$$

$$H = \frac{C_0 - C_e}{C_0} \times 100$$

Where:  $C_0$ ,  $C_e$  are the initial ciprofloxacin concentration and the remaining ciprofloxacin concentration after adsorption in the solution (mg/L), respectively;  $m$  is the mass of the material used (g);  $V$  is the volume of the solution (L).

## Results and discussion

### Material Characteristics of Biochar

The FTIR spectra of pine bark-derived biochar synthesized by microwave-assisted pyrolysis are shown in Figure 1.

In Figure 1a, a broad band at  $3384.8$   $\text{cm}^{-1}$  indicates O–H groups, while peaks at  $2920.4$   $\text{cm}^{-1}$  and  $1384.5$   $\text{cm}^{-1}$  correspond to C–H vibrations in methylene groups and cellulose. Strong peaks at  $1575.5$   $\text{cm}^{-1}$  and  $1165.4$   $\text{cm}^{-1}$  are due to aromatic C=C and C–O/C–O–C stretching [7]. In addition, a sharp signal at  $877.5$   $\text{cm}^{-1}$  may be assigned to the out-of-plane bending vibration of C–H in aromatic compounds. The peak at  $1435.5$   $\text{cm}^{-1}$  is likely due to the bending vibration of C–OH in cellulose or asymmetric stretching of methylene groups or C–H bonds in cellulose and lignin [8].

After microwave pyrolysis (Figure 1b), a weaker O–H peak appears at  $3442.5$   $\text{cm}^{-1}$ , along with weak signals at  $2896.4$   $\text{cm}^{-1}$  (C–H) and  $2335.7$   $\text{cm}^{-1}$  ( $\text{CO}_2$ ), indicating decomposition of cellulose and  $\text{CO}_2$  adsorption. The presence of  $\text{CO}_2$  in the IR spectrum also implies that  $\text{CO}_2$  may have been adsorbed onto the biochar surface during the process, which may be indicative of a high specific surface area of the material [8,9].

A sharp peak at  $1580.3$   $\text{cm}^{-1}$  is attributed to C=O or aromatic C=C stretching, while peaks at  $1387.7$  and  $1150.5$   $\text{cm}^{-1}$  indicate methylene/methyl vibrations and aromatic structures [10].

Overall, the spectra confirm the formation of polyaromatic structures with residual hydroxyl and carbonyl groups. Microwave-assisted pyrolysis enhances graphitic character and hydrophobicity, potentially improving the material's adsorption performance [11].

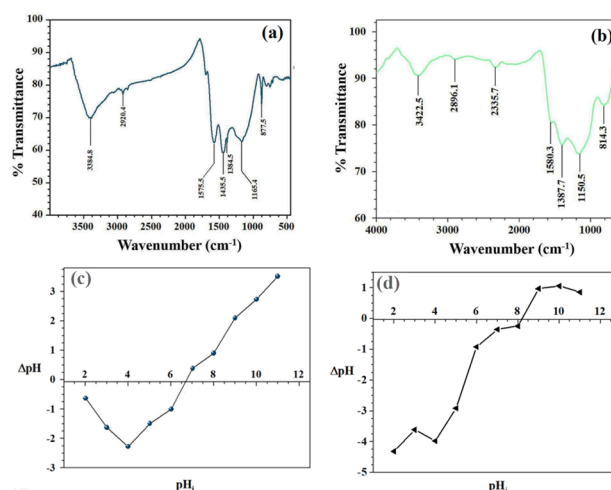


Fig 1: FTIR spectra of biochar before (a) and after (b) microwave pyrolysis. Point of zero charge ( $\text{pH}_{\text{pzc}}$ ) plot of biochar before (c) and after (d) microwave-assisted pyrolysis.

The surface of the material can carry either a positive or negative charge in aqueous environments, depending on the solution pH and the material's surface characteristics [12]. The determination of the point of zero charge ( $\text{pH}_{\text{pzc}}$ ) revealed that the value increased from approximately 6.7 before microwave pyrolysis to 8.3 after treatment. This shift indicates a significant alteration in surface chemistry: acidic oxygen-containing groups (–COOH, –OH phenolic) were decomposed during pyrolysis, while more basic sites such as carbonyl, pyridinic moieties, or electron-rich domains on the carbon framework were generated. Consequently, the surface of the material became more basic after microwave treatment. This change plays an important

role in the adsorption of ciprofloxacin. At near-neutral pH (6–8), ciprofloxacin mainly exists in the zwitterionic form ( $\text{CIP}^{\pm}$ ), carrying both positive and negative charges. Under these conditions, the post-pyrolysis material (positively charged at  $\text{pH} < 8.3$ ) can establish favorable electrostatic interactions with the negatively charged carboxylate group of CIP, while maintaining additional adsorption mechanisms such as hydrogen bonding and  $\pi$ – $\pi$  interactions between the aromatic rings of the antibiotic and the carbon framework. In contrast, the pre-pyrolysis material ( $\text{pH}_{\text{pzc}} = 6.7$ ) is already negatively charged at neutral pH, which reduces electrostatic attraction with the CIP molecules. Therefore, the increased  $\text{pH}_{\text{pzc}}$  after microwave pyrolysis contributes to the enhanced adsorption performance toward ciprofloxacin under near-neutral conditions, which are typical of real wastewater treatment systems [13].

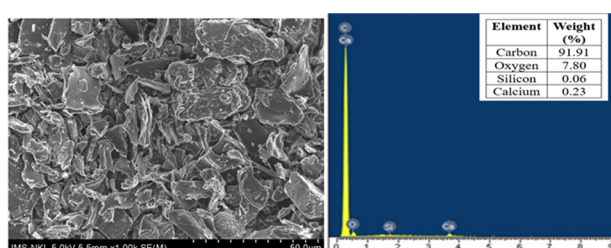


Fig 2: SEM images and EDX spectra of BCMAP

The SEM image in Figure 2 shows that the material consists of thin, porous, and irregularly dispersed fragments, indicating the breakdown of the original biomass structure after pyrolysis. The surface appears rough and heterogeneous. The biochar particles exhibit a wrinkled and uneven surface, which may provide numerous active sites favorable for adsorption. Some fragments display flake-like structures with small cracks, suggesting the development of porous networks or microporous systems during the microwave-assisted pyrolysis process [14].

The EDX spectrum (Figure 2) shows that BCMAP biochar is mainly composed of carbon (91.91%) and oxygen (7.80%), indicating effective carbonization and the presence of oxygen-containing functional groups. Minor amounts of calcium (0.23%) and silicon (0.06%) suggest residual inorganic matter from the raw material. The high carbon content and low ash confirm successful conversion of pine bark into carbon-rich biochar, suitable for environmental applications like adsorption [15]. The BCMAP biochar exhibited a high specific surface area of  $592.320 \text{ m}^2/\text{g}$  and a pore volume of  $0.197 \text{ cm}^3/\text{g}$ , which were significantly improved compared to the precursor material before microwave pyrolysis ( $338.533 \text{ m}^2/\text{g}$  and  $0.139 \text{ cm}^3/\text{g}$ , respectively).

<https://doi.org/10.62239/jca.2025.033>

These values suggest that microwave-assisted pyrolysis effectively enhanced the material's porosity by promoting rapid gas release and the formation of well-developed pore networks [6].

### Investigation of factors affecting the adsorption of ciprofloxacin onto biochar prepared by microwave-assisted pyrolysis

Ciprofloxacin has two  $\text{pK}_a$  values: 5.8 (carboxyl group) and 8.89 (amine group in the piperazine ring), meaning its form varies with pH—cationic ( $\text{pH} < 5.8$ ), zwitterionic ( $\text{pH} 5.8\text{--}8.89$ ), or anionic ( $\text{pH} > 8.89$ ). pH also affects the surface charge of biochar, making it a key factor in adsorption. As shown in Figure 3a, ciprofloxacin adsorption on BCMAP increased from pH 2 to 6 (maximum 90.97%), then declined. This trend is due to reduced electrostatic repulsion in the zwitterionic form and minimized competition with  $\text{H}^+$  or  $\text{OH}^-$  ions at near-neutral pH [16]. Moreover, the pH effect can also be explained based on the point of zero charge ( $\text{pH}_{\text{pzc}}$ ) of the material. The  $\text{pH}_{\text{pzc}}$  of the material was determined to be approximately 8.3, meaning that at  $\text{pH} < 8.3$ , the surface of the material is positively charged and favors the adsorption of anionic species—specifically the negatively charged part of the zwitterionic  $\text{CFC}^{\pm}$ . Conversely, at  $\text{pH} > 8.3$ , the surface becomes negatively charged and preferentially adsorbs cationic species, i.e., the positively charged portion of the zwitterion. Therefore, pH 6 was selected for use in subsequent adsorption experiments [10].

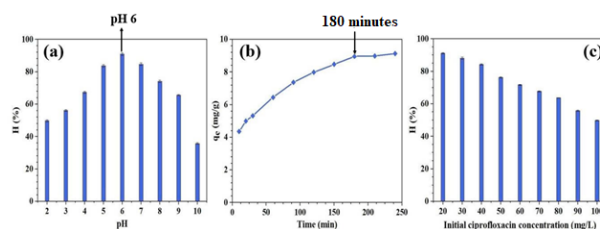


Fig 3: Effect of pH (a), contact time (b), and initial concentration (c) on the adsorption of ciprofloxacin onto BCMAP

The effect of contact time on the adsorption of ciprofloxacin onto BCMAP (Figure 3b) shows that the adsorption capacity increases rapidly between 10 and 180 minutes and gradually levels off, with no significant change observed from 180 to 240 minutes. This indicates that the adsorption process had reached equilibrium. Therefore, an equilibrium contact time of 180 minutes was selected for use in subsequent experiments.

The results of the effect of initial ciprofloxacin concentration on the adsorption efficiency of BCMAP

show that the adsorption efficiency decreases as the initial antibiotic concentration increases. This decrease in efficiency can be explained by the fact that the mass of BMAP used in the experiments remained constant; thus, the number of available adsorption sites was fixed. At low ciprofloxacin concentrations, the number of antibiotic molecules is relatively small, allowing for nearly complete adsorption, resulting in high efficiency. However, at higher concentrations, the number of ciprofloxacin molecules exceeds the available adsorption sites on the biochar surface, leaving a significant portion of the antibiotic unadsorbed, thereby reducing the overall adsorption efficiency [17].

### Adsorption Kinetics Study

The study of ciprofloxacin adsorption kinetics onto BMAP is crucial as it provides insights into the adsorption mechanism and the rate at which the process occurs. In this study, the adsorption of ciprofloxacin onto the material was evaluated using two widely applied kinetic models: the pseudo-first-order and pseudo-second-order kinetic models.

The integrated form of the pseudo-first-order kinetic equation is:  $\lg(q_e - q_t) = \lg q_e - \frac{k_1 \times t}{2.303}$

The integrated form of the pseudo-second-order kinetic equation is:  $\frac{t}{q_t} = \frac{1}{k_2 q_e^2} + \left(\frac{1}{q_e}\right) \times t$

Where:

$q_e$  is the adsorption capacity at equilibrium (mg/g),

$q_t$  is the adsorption capacity at time  $t$  (mg/g),

$k_1$  is the pseudo-first-order rate constant ( $\text{min}^{-1}$ ),

$k_2$  is the pseudo-second-order rate constant ( $\text{g} \cdot \text{mg}^{-1} \cdot \text{min}^{-1}$ ).

Based on the experimental data, linear plots of  $\log(q_e - q_t)$  versus  $t$  (for the pseudo-first-order model) and  $t/q_t$  versus  $t$  (for the pseudo-second-order model) were constructed. The kinetic parameters were calculated from the slope and intercept of the respective linear plots and are presented in Table 1.

Table 1. Kinetic parameters for the adsorption of ciprofloxacin onto BMAP.

Kinetic Model	Parameter	Value ( $\pm$ SD)
Pseudo-first-order model	$R^2$	$0.9729 \pm 0.0077$
	$q_{e,cal}$ (mg/g)	$6.6085 \pm 0.0004$
	$k_1$ ( $\text{min}^{-1}$ )	$0.0029 \pm 0.0002$
$q_{e,exp}$ (mg/g)		9.27
Pseudo-second-order model	$k_2$ ( $\text{g}/(\text{mg} \cdot \text{min})$ )	$0.0042 \pm 0.0001$
	$q_{e,cal}$ (mg/g)	$9.9282 \pm 0.0500$
	$R^2$	$0.9945 \pm 0.0004$

The adsorption kinetics of ciprofloxacin onto BMAP were better described by the pseudo-second-order model, as evidenced by the higher correlation coefficient ( $R^2 = 0.9945$ ) compared to the pseudo-first-order model ( $R^2 = 0.9729$ ). Additionally, the calculated equilibrium adsorption capacity from the pseudo-second-order model ( $q_{e,cal} = 9.93$  mg/g) closely agrees with the experimental value ( $q_{e,exp} = 9.27$  mg/g), further confirming that the adsorption process likely follows a chemisorption mechanism [12].

### Adsorption Isotherm Study of Ciprofloxacin on BMAP

The study of ciprofloxacin adsorption isotherms on BMAP provides insights into the relationship between the amount of ciprofloxacin adsorbed onto the material and its equilibrium concentration in aqueous solution. In this study, both the Freundlich and Langmuir isotherm models were applied to describe the adsorption behavior of ciprofloxacin on the biochar.

The Freundlich isotherm model is an empirical equation suitable for adsorption on heterogeneous surfaces. Its linearized form is:  $\lg q_e = \lg K_F + \frac{1}{n} \times \lg C_e$

The Langmuir isotherm model assumes monolayer adsorption on a surface with a finite number of identical and energetically equivalent adsorption sites. The linearized Langmuir equation is expressed as:

$$\frac{C_e}{q_e} = \frac{C_e}{q_{max}} + \frac{1}{q_{max} \times K_L}$$

Where:

$q_e$  (mg/g): adsorption capacity at equilibrium,

$q_{max}$  (mg/g): maximum monolayer adsorption capacity,

$C_e$  (mg/L): equilibrium concentration of ciprofloxacin,

$K_L$  (L/mg): Langmuir constant related to the affinity of binding sites,

$K_F$  and  $1/n$ : Freundlich constants indicating adsorption capacity and intensity.

The dimensionless separation factor ( $R_L$ ) is used to assess the favorability of ciprofloxacin adsorption and is calculated as:  $R_L = \frac{1}{1 + K_L \times C_0}$

Interpretation of  $R_L$  values:

$R_L = 0$ : irreversible adsorption,  $R_L > 1$ : unfavorable adsorption,  $0 < R_L < 1$ : favorable adsorption,  $R_L = 1$ : linear adsorption. The adsorption isotherm study was carried out by varying the initial ciprofloxacin concentration (10–100 mg/L), with a constant adsorbent mass (0.1000 g), while pH and contact time were kept constant as optimized in previous experiments. The equilibrium adsorption results are presented in Table 3.

Table 3. Isotherm parameters for ciprofloxacin adsorption onto BCMAP biochar

Isotherm Model	Parameter	Value ( $\pm$ SD)
Langmuir model	$q_{\max}$ (mg/g)	$26.51 \pm 0.21$
	$K_L$ (L/mg)	$0.2906 \pm 0.0181$
	$R_L$	$0.1471 \pm 0.0079$
	$R^2$	$0.9925 \pm 0.0009$
Freundlich model	KF	$5.8575 \pm 0.2318$
	$1/n$	$0.3008 \pm 0.0085$
	$R^2$	$0.9379 \pm 0.0033$

The Langmuir adsorption model provides a better fit to the experimental data compared to the Freundlich model, as indicated by the higher correlation coefficient ( $R^2 = 0.9925$ ). The calculated separation factor ( $R_L = 0.1471$ ) falls within the range of 0 to 1, suggesting that the adsorption of ciprofloxacin onto BCMAP is favorable. The maximum monolayer adsorption capacity ( $q_{\max}$ ) was determined to be 26.51 mg/g, confirming the material's efficiency in single-layer adsorption processes [18].

Although the Freundlich constant  $1/n = 0.3008$  (less than 1) also implies favorable adsorption, the lower correlation coefficient ( $R^2 = 0.9379$ ) indicates that the Freundlich model offers a less accurate representation of the experimental data when compared to the Langmuir model. This suggests that the adsorption process is likely monolayer and occurs on a homogeneous surface [19].

## Conclusion

Biochar was successfully synthesized from pine bark using microwave-assisted pyrolysis (BCMAP) within 10 minutes at a power of 800 W.

The physicochemical characteristics of BCMAP were determined using FT-IR, SEM, EDX, and BET analysis. The point of zero charge ( $pH_{pzc}$ ) of BCMAP was found to be 8.3, with a specific surface area and pore volume of 592.320 m<sup>2</sup>/g and 0.197 cm<sup>3</sup>/g, respectively.

The main factors affecting the adsorption efficiency of ciprofloxacin onto BCMAP include solution pH, contact time, and initial antibiotic concentration. The highest adsorption efficiency of 90.97% was achieved at pH 6, contact time of 180 minutes, and an initial concentration of 20 mg/L.

The adsorption kinetics were best described by the pseudo-second-order kinetic model, with a correlation coefficient  $R^2 = 0.9925$ . The Langmuir isotherm model

provided the best fit for the equilibrium data, with a calculated maximum adsorption capacity of 26.51 mg/g. Additionally, the Freundlich isotherm model yielded a  $1/n$  value of less than 1, indicating favorable adsorption and suggesting that the process followed a physical adsorption mechanism.

## Acknowledgments

This research is funded by Vietnam Ministry of Education and Training under grant number B2025-DLA-01

## References

1. D. Torumkunev, S. Kundu, G.V. Vu, H.A. Nguyen, H.V. Pham, P. Kamble, N.T. Ha Lan, N. Keles, J. Antimicrob. Chemother., 77 (2022) i26. <https://doi.org/10.1093/jac/dkac214>
2. D.C. Hooper, G.A. Jacoby, Ann. N. Y. Acad. Sci., 1354 (2015) 12. <https://doi.org/10.1111/nyas.12830>
3. B.J. Langford, M. So, S. Raybardhan, V. Leung, D. Westwood, D.R. MacFadden, J.-P.R. Soucy, N. Daneman, Clin. Microbiol. Infect., 27 (2021) 583. <https://doi.org/10.1016/j.cmi.2020.07.016>
4. M. Patel, R. Kumar, K. Kishor, T. Mlsna, C.U. Pittman Jr., D. Mohan, Chem. Rev., 119 (2019) 3510. <https://doi.org/10.1021/acs.chemrev.8b00299>
5. A. Orjuela, A.J. Yanez, A. Santhanakrishnan, C.T. Lira, D.J. Miller, Chem. Eng. J., 223 (2012) 504. <https://doi.org/10.1016/j.cej.2012.01.103>
6. Y. Zhang, S. Fan, T. Liu, W. Fu, B. Li, Sustain. Energy Technol. Assess., 50 (2022) 101873. <https://doi.org/10.1016/j.seta.2021.101873>
7. A.U. Štefanko, D. Leszczynska, Front. Energy Res., 8 (2020) 138. <https://doi.org/10.3389/fenrg.2020.00138>
8. B. Handiso, T. Pääkkönen, B.P. Wilson, Waste Manag. Bull. 2(4) (2024) 281–287. <https://doi.org/10.1016/j.wmb.2024.11.008>
9. H. Wang, Y. Yang, M. Wang, R. Yuan, W. Song, L. Wang, N. Liang, J. Shi, J. Li, Sustainability, 16(7) (2024) 2629. <https://doi.org/10.3390/su16072629>
10. T. Atugoda, C. Gunawardane, M. Ahmad, M. Vithanage, Chemosphere, 281 (2021) 130676. <https://doi.org/10.1016/j.chemosphere.2021.130676>
11. Y.-F. Huang, P.-T. Chiueh, S.-L. Lo, Sustain. Environ. Res., 26 (2016) 103. <https://doi.org/10.1016/j.serj.2016.04.012>
12. G. Murtaza, Z. Ahmed, D.-Q. Dai, R. Iqbal, S. Bawazeer, M. Usman, M. Rizwan, J. Iqbal, M.I. Akram, A.S. Althubiani, A. Tariq, I. Ali, Front. Environ. Sci., 10 (2022) 1035865. <https://doi.org/10.3389/fenvs.2022.1035865>
13. C. Banik, M. Lawrinenko, S. Bakshi, D.A. Laird, J. Environ. Qual., 47 (2018) 452. <https://doi.org/10.2134/jeq2017.11.0432>

14. Z.U. Zango, A. Garba, A. Haruna, S.S.I. Imam, A.U. Katsina, A.F. Ali, A. Zainal Abidin, M.U. Zango, Z.N. Garba, A. Hosseini-Bandegharaei, A.U. Yuguda, H. Adamu, J. Water Process Eng., 67 (2024) 106186. <https://doi.org/10.1016/j.jwpe.2024.106186>
15. H. Liu, G. Xu, G. Li, Sci. Total Environ., 747 (2020) 141492. <https://doi.org/10.1016/j.scitotenv.2020.141492>
16. S. Mirizadeh, D.S.A. Arni, M. Elwaheidi, A.A.M. Salih, A. Convert, A.A. Casazza, Chem. Eng. Technol., 46 (2023). <https://doi.org/10.1002/ceat.202300193>
17. Y. Xue, Y. Guo, X. Zhang, M. Kamali, T.M. Aminabhavi, L. Appels, R. Dewil, Chem. Eng. J., 450 (2022) 137896. <https://doi.org/10.1016/j.cej.2022.137896>
18. R. Huang, Q. Zhu, W. Wanga, Y. Hua, New J. Chem., 47 (2023) 7910. <https://doi.org/10.1039/D3NJ00403A>
19. P. Zhang, Y. Li, H. Qi, X. Li, ChemistrySelect, 8 (2023) e202302116. <https://doi.org/10.1002/slct.202302116>